Available online at www.sciencedirect.com
ScienceDirect
Trans. Nonferrous Met. Soc. China 32(2022) 1314−1324

Transactions of
Nonferrous Metals
Society of China
www.tnmsc.cn

Enhancement of $CaMoO_4$ calcine decomposition and recovery of calcium resource by HCl cycle leaching

Li ZENG[1,2,3], Man WANG[1,2,3], Chao XIAO[1,2,3], Sheng-xi WU[1,2,3],
Gui-qing ZHANG[1,2,3], Wen-juan GUAN[1,2,3], Qing-gang LI[1,2,3], Zuo-ying CAO[1,2,3]

1. School of Metallurgy and Environment, Central South University, Changsha 410083, China;
2. Key Laboratory of Metallurgical Separation Science and Engineering of Non-ferrous Metals Industry,
Central South University, Changsha 410083, China;
3. National Engineering Laboratory for Efficient Utilization of Refractory Non-ferrous Metals Resources,
Central South University, Changsha 410083, China

Received 3 April 2021; accepted 10 September 2021

Abstract: The thermodynamic equilibrium diagrams of $CaMoO_4-CaSO_4-H_2SO_4-H_2O$, $CaMoO_4-HCl-H_2O$ and $CaSO_4-CaCl_2-HCl-H_2O$ systems at 298 K were established. The calculation results demonstrated that HCl displays a much higher solubility of $CaSO_4$ than H_2SO_4. The leaching mechanism of Mo from $CaMoO_4$ calcine was systematically investigated from the perspective of the micro particle properties variation. HCl exhibits an excellent leaching performance for Mo from $CaMoO_4$ calcine due to the elimination of surface coating and the dissolution of a mass of Mo embedded in $CaSO_4$ matrix. Excellent Mo leaching efficiency of 99.7% was achieved under the optimal conditions of decomposing $CaMoO_4$ calcine by 2.4 mol/L HCl with a liquid/solid ratio of 10:1 at 50 °C for 60 min. Based on the experimental results, a highly efficient and green cycle leaching process of molybdenum from molybdenite was proposed, which eliminated surface coating and physical entraining, and converted most of the calcium from $CaMoO_4$ calcine into high purity gypsum by-product.

Key words: calcium molybdate; molybdenum; H_2SO_4 leaching; HCl leaching; thermodynamics

---

1 Introduction

Molybdenum (Mo) is a strategic metal element due to its critical application in the catalyst industry and the cemented carbide alloy tool which is called as the “tooth” of the industry [1]. In molybdenite ore, the only significant commercial molybdenum resource explored at present, Mo, majorly occurs as MoS_2 and the content of Mo is 30%−40% [2,3]. On the other hand, the proportion of Mo recovered from secondary resources such as spent catalysts (in the form of MoS_2) is going through a rapid growing [4−6]. MoS_2 in these resources can hardly be decomposed by mineral acids under ordinary conditions. Therefore, in industrial practice oxidating roasting was proposed to break the mineral crystal structure of MoS_2 for Mo leaching [7,8]. However, direct oxidating roasting with air or oxygen would generate huge amount of toxic SO_2 gas. To eliminate the emission of SO_2, the CaO roasting method which converts MoS_2 to $CaMoO_4$ and solidifies S as $CaSO_4$ has been widely applied in Mo metallurgical industry. But issues of calcium sulphate coating and high loss of Mo in residue are still faced by the leaching of Mo from the molybdenite calcine ($CaMoO_4$, calcium molybdate). Then, it is of critical importance to enhance the dissolution of $CaMoO_4$ calcine in a green way.

$CaMoO_4$ can be decomposed by solutions of

Corresponding author: Sheng-xi WU, E-mail: csuwushengxi@126.com

DOI: 10.1016/S1003-6326(22)65876-X

Na_2CO_3, phosphates and mineral acids [9,10]. SONG et al [11] achieved a 99.7% decomposition efficiency of $CaMoO_4$ by 12% Na_2CO_3 solution at 80 °C for 2 h. XIA et al [12] reported that an increasing concentration of Na_2CO_3 promoted the decomposition of $CaMoO_4$. PAN and ZHU [13] achieved a 94% leaching efficiency of Mo by pressed leaching with 100 g/L Na_2CO_3 at 180 °C for 1 h. However, for Na_2CO_3 leaching process, a complete decomposition requires much excessive Na_2CO_3 and elevated temperature, resulting in high concentration of free base in leach solutions and difficult downstream treatments. ZHANG et al [14] found that phosphates exhibited better performance than Na_2CO_3 for $CaMoO_4$ decomposition, but a significant amount of phosphorus was introduced and difficult to be removed. The decomposition of $CaMoO_4$ with alkaline and phosphate solutions did not break the abundant $CaSO_4$ matrix and limited the effective diffusion of leachant and the generated ions.

Recently, the decomposition of $CaMoO_4$ with acids has also been considered as a promising alternative [15,16]. The leaching conditions for $CaMoO_4$ decomposition with acids are much milder than those with alkali, generally at normal temperature and pressure [17−19]. ILHAN et al [20,21] decomposed $CaMoO_4$ by oxalic acid and Mo was leached as soluble $H_2[(MoO_3)_2(C_2O_4)]$, but the surface coating of undissolved particles by the generated CaC_2O_4 retarded further decomposition of $CaMoO_4$. SINGH et al [22] leached 99% of Mo using 1−2 mol/L H_2SO_4 by double-leaching $CaMoO_4$ at 80−90 °C for 2 h. ZOU and ZHOU [23] leached 98.5% of Mo from $CaMoO_4$ by using 5 vol.% H_2SO_4 with a liquid/solid (L/S) ratio of 3:1 at 90 °C for 2 h. However, in H_2SO_4 leaching, the undissolved $CaSO_4$ matrix embedded with Mo and the coating caused by the generated $CaSO_4$ results in a slow leaching kinetics, huge amount of leach residue and high loss of Mo in residue [24]. To solve these problems, a novel process including HCl leaching, Mo extraction with HEHEHP and HCl regeneration was proposed. In this process, a higher recovery of Mo can be anticipated since the passivation caused by $CaSO_4$ is eliminated and the volume of solid waste is significantly reduced by transferring most $CaSO_4$ into a useful by-product. However, the leaching of Mo from calcium molybdate (embedded with $CaSO_4$) with HCl has rarely been reported, and whether the generated H_2MoO_4 led to an obvious passivation is still unknown.

To enhance the decomposition of $CaMoO_4$ calcine and recover calcium as gypsum by-product, in this study, thermodynamic analysis on acid decomposition of $CaMoO_4$ was investigated. Then, the effects of acid concentration, temperature, time, L/S ratio, and $CaCl_2$ concentration on the leaching efficiency of Mo from $CaMoO_4$ with HCl were studied. And the overall recovery of Mo in the process of HCl leaching—Mo extraction—HCl regeneration process was examined.

2 Thermodynamic analysis

The ionic compositions in $CaMoO_4$−$CaSO_4$−H_2SO_4−H_2O and $CaMoO_4$−HCl−H_2O aqueous solution systems consist of MoO_4^{2-}, $H_2MoO_{4(aq)}$, $HMoO_4^-$, MoO_2^{2+}, MoO_2OH^+, Ca^{2+}, $CaOH^+$, $Ca(OH)_{2(aq)}$, H_2SO_4, HSO_4^-, SO_4^{2-}, HCl, Cl^-, H^+ and OH^-, and the solid phases include $H_2MoO_{4(s)}$, $CaMoO_{4(s)}$ and $CaSO_{4(s)}$. The equilibrium constants (lg K) of reactions were listed in Table 1.

Thermodynamic analysis was conducted according to the data in Table 1. Generally, in metallurgical engineering, for solutions with a high concentration of metal ions, the concentration was used instead of the activity. The mathematical relationships of the species can be expressed as equations below:

$$[H^+]^2[MoO_4^{2-}]=10^{-13.33} \tag{14}$$

$$[H_2MoO_{4(aq)}]=10^{6.85}[H^+]^2[MoO_4^{2-}] \tag{15}$$

$$[HMoO_4^-]=10^{5.01}[H^+][MoO_4^{2-}] \tag{16}$$

$$[MoO_2^{2+}]=10^{8.33}[H^+]^4[MoO_4^{2-}] \tag{17}$$

$$[MoO_2OH^+]=10^{7.88}[H^+]^3[MoO_4^{2-}] \tag{18}$$

$$[Ca^{2+}][MoO_4^{2-}]=10^{-8.55} \tag{19}$$

$$[Ca^{2+}][SO_4^{2-}]=10^{-5.04} \tag{20}$$

$$[Ca(OH)_{2(aq)}]=10^{2.77}[Ca^{2+}][OH^-]^2 \tag{21}$$

$$[CaOH^+]=10^{1.4}[Ca^{2+}][OH^-] \tag{22}$$

$$[H_2SO_4]=10^{-3}[H^+][HSO_4^-] \tag{23}$$

$$[HSO_4^-]=10^{1.92}[H^+][SO_4^{2-}] \tag{24}$$

Table 1 Equilibrium reactions and equilibrium constants (lg *K*) of $CaMoO_4$−$CaSO_4$−H_2SO_4−H_2O and $CaMoO_4$−HCl−H_2O systems at 298 K

Equilibrium reaction	Equilibrium constant, lg *K*	Equation No.	Reference
$H_2MoO_{4(s)}=2H^++MoO_4^{2-}$	−13.33	(1)	[25]
$H_2MoO_{4(aq)}=2H^++MoO_4^{2-}$	−6.85	(2)	[25]
$HMoO_4^-=H^++MoO_4^{2-}$	−5.01	(3)	[25]
$MoO_2^{2+}+2H_2O=4H^++MoO_4^{2-}$	−8.33	(4)	[25]
$MoO_2OH^++H_2O=3H^++MoO_4^{2-}$	−7.88	(5)	[25]
$CaMoO_{4(s)}=Ca^{2+}+MoO_4^{2-}$	−8.53	(6)	[14]
$CaSO_{4(s)}=Ca^{2+}+SO_4^{2-}$	−5.04	(7)	[26]
$Ca^{2+}+2OH^-=CaOH_{2(aq)}$	2.77	(8)	[26]
$Ca^{2+}+OH^-=CaOH^+$	1.4	(9)	[26]
$H_2SO_4=H^++HSO_4^-$	3	(10)	[26]
$HSO_4^-=H^++SO_4^{2-}$	−1.92	(11)	[26]
$HCl=H^++Cl^-$	8.0	(12)	[26]
$H_2O=H^++OH^+$	−14.0	(13)	[26]

$$[HCl]=10^{-8}[H+][Cl^-] \tag{25}$$

$$[H^+][OH^-]=10^{-14} \tag{26}$$

The total concentrations of Ca, Mo, S and Cl in aqueous solution were calculated according to Eqs. (27)−(30), separately:

$$[Ca]_T=[Ca^{2+}]+[CaOH^+]+[Ca(OH)_{2(aq)}] \tag{27}$$

$$[Mo]_T=[MoO_4^{2-}]+[H_2MoO_{4(aq)}]+[HMoO_4^-]+[MoO_2^{2+}]+[MoO_2OH^+] \tag{28}$$

$$[S]_T=[SO_4^{2-}]+[HSO_4^-]+[H_2SO_4] \tag{29}$$

$$[Cl]_T=[Cl^-]+[HCl] \tag{30}$$

According to the equations above, the thermodynamic analysis on $CaMoO_4$−H_2SO_4−H_2O and $CaMoO_4$−HCl−H_2O systems was carried out to demonstrate the feasibility on decomposition of calcium molybdate using the sulfuric and hydrochloric acids.

In the aqueous solution system of $CaSO_4$−$CaCl_2$−HCl−H_2O, sulphur presents in forms of H_2SO_4, HSO_4^- and SO_4^{2-}. Their concentration depends on the degree of the ionization process of $CaSO_{4(s)}$. Then, the dissolution concentration of $CaSO_{4(s)}$ in solution can be expressed as Eq. (31):

$$[CaSO_4]_D=[H_2SO_4]+[HSO_4^-]+[SO_4^{2-}] \tag{31}$$

In addition, the equilibrium of charge in $CaSO_4$−$CaCl_2$−HCl−H_2O system can be expressed as Eq. (32):

$$2[Ca^{2+}]+2[H^+]+[CaOH^+]=2[SO_4^{2-}]+[HSO_4^-]+[OH^-]+[Cl^-] \tag{32}$$

Based on Eqs. (31) and (32), the thermodynamic study with the system of $CaSO_4$−$CaCl_2$−HCl−H_2O was conducted to investigate the effects of $CaCl_2$ and HCl concentrations on the solubility of $CaSO_4$.

2.1 Thermodynamic analysis of $CaMoO_4$−$CaSO_4$−H_2SO_4−H_2O and $CaMoO_4$−HCl−H_2O systems

The lg *c*−pH diagrams of $CaMoO_4$−$CaSO_4$−H_2SO_4−H_2O and $CaMoO_4$−HCl−H_2O systems at equilibrium are drawn in Fig. 1. As shown in Fig. 1(a), the total Ca^{2+} concentration maintained at a low level in the whole pH range, indicating that only small amount of calcium can be leached in the case of $CaMoO_4$ decomposition with H_2SO_4. The molar ratios of $CaSO_{4(s)}$ to $CaMoO_{4(s)}$ and $H_2MoO_{4(s)}$ to $CaMoO_{4(s)}$ were 1.142 (52.16/45.66) and 1.136 (51.86/45.66), respectively, indicating that the surface of $CaMoO_{4(s)}$ could be easily wrapped by $CaSO_{4(s)}$ and $H_2MoO_{4(s)}$ during the decomposition process, resulting in incomplete decomposition of $CaMoO_{4(s)}$ by H_2SO_4. Data in Fig. 1(b) demonstrated that the Ca^{2+} solubility in HCl was 100 times higher than that in H_2SO_4.

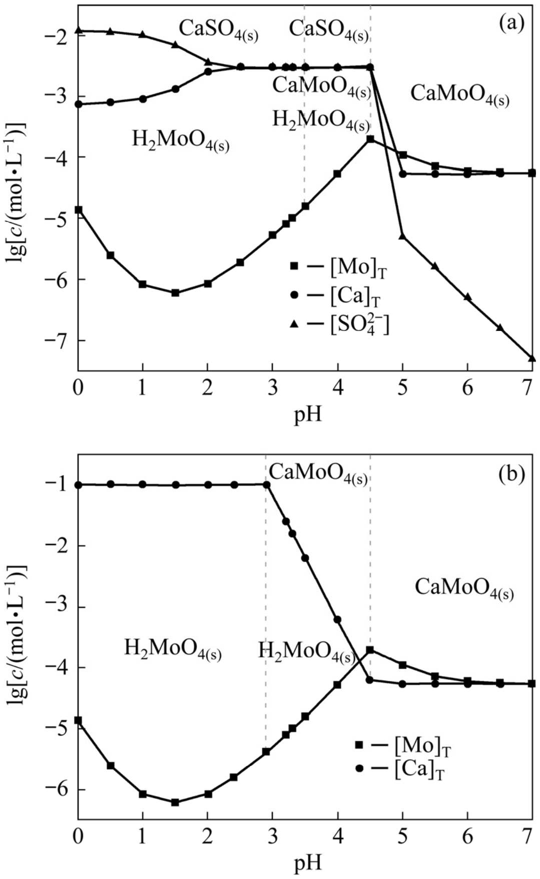

Fig. 1 lg c–pH diagrams of $CaMoO_4$−$CaSO_4$−H_2SO_4−H_2O (a) and $CaMoO_4$−HCl−H_2O (b) systems at 298 K

The effect of L/S ratio on the decomposition of $CaMoO_4$ with HCl was simulated and displayed in Fig. 2. The terminal pH of decomposition reduced from 2.90 to 2.60 with the decrease in L/S ratio from 10:1 to 2:1 when the initial pH is kept constant. This could be attributed to the increase of Ca^{2+} concentration in leach solutions that retarded further decomposition of $CaMoO_{4(s)}$ since surface coating caused by the generated $H_2MoO_{4(s)}$ occurred on some of $CaMoO_4$ particles. But fortunately, the H_2MoO_4 solubility can be significantly increased by increasing the HCl concentration (as shown in Table 2), then reduced the resistance of mass transfer and increased the decomposition efficiency of $CaMoO_{4(s)}$.

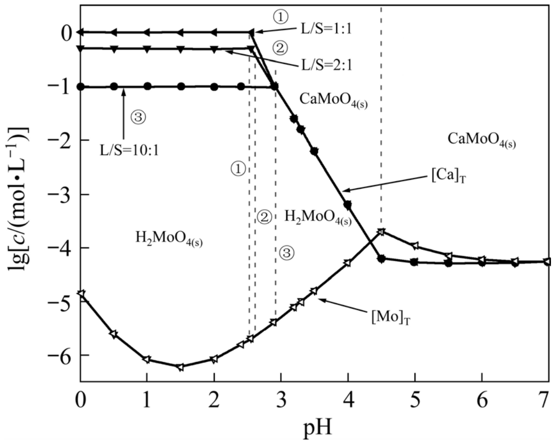

Fig. 2 Effect of L/S ratio on decomposition of $CaMoO_4$ with HCl

Table 2 Solubility of molybdate in HCl solution

HCl concentration/ $(g\cdot L^{-1})$	Solubility of $H_2MoO_4/(g\cdot L^{-1})$		
	20 °C	50 °C	70 °C
40	3.8	2.46	4.6
80	10.9	6.48	13
130	29.2	18.6	42.6
200	101.5	124.5	135.9
270	192.6	270.5	265
400	440	551.3	535.6

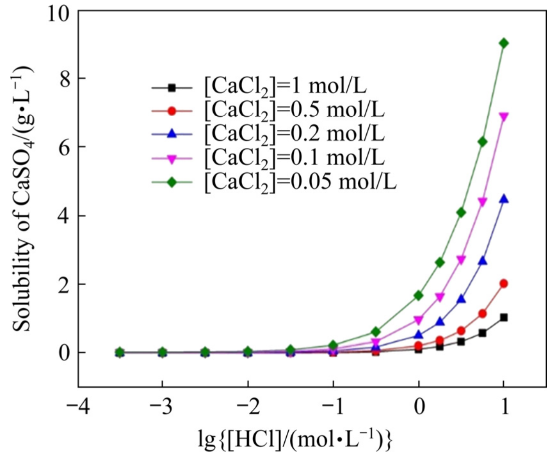

Fig. 3 Effects of HCl and $CaCl_2$ concentrations on solubility of $CaSO_4$ in $CaSO_4$−$CaCl_2$−HCl−H_2O system

2.2 Thermodynamic analysis of $CaSO_4$−$CaCl_2$−HCl−H_2O system

As the curves in Fig. 3 demonstrated, the solubility of $CaSO_4$ increased with the increase of acidity since the increased acidity ($[H^+]$) dissolved $CaSO_4$ by forming HSO_4^- and released Ca^{2+} [27,28]. However, the increase of $CaCl_2$ concentration obviously reduced the solubility of $CaSO_4$. For example, the solubility of $CaSO_4$ decreased from 2.64 to 0.185 g/L with the increase in $CaCl_2$ concentration from 0.05 to 1.0 mol/L with 1.77 mol/L HCl. According to the solubility constant of $CaSO_4$, the increase in Ca^{2+} concentration results in the decrease of SO_4^{2-}

concentration, and therefore the decrease of $CaSO_4$ solubility.

3 Experimental

3.1 Materials

A sample of molybdenite containing 41 wt.% Mo was provided by a native plant in China and all other chemicals used in this study were of chemical grade, provided by Beijing Chemical Reagent Co., Ltd., and Xilong Chemical Co., Ltd. After roasting with $Ca(OH)_2$ at CaO/MoS_2 molar ratio of 3:1 and 650 °C for 2 h, the $CaMoO_4$ calcine was obtained as raw material for acid leaching tests. The oxidation (retention) of molybdenum reached 99.3% with the sulphur fixation of 98.2%. The composition of the $CaMoO_4$ calcine is shown in Table 3 and the XRD patterns before and after roasting of molybdenite with lime are presented in Figs. 4(a) and (b). It is noted that only two macro phases, $CaMoO_4$ and $CaSO_4$, are found in the calcine. The occurrence of $CaMoO_4$ and $CaSO_4$ in calcine is simply characterized by SEM−EDS (Figs. 4(c, d)), indicating that these two phases are deeply embedded in each other.

3.2 Experimental operations

For each test of leaching, a sample of 20 g $CaMoO_4$ calcine was taken and placed in a 500 mL beaker immersed in a water bath. The mixed solution of concentrate HCl and water was then added into the beaker and mixed with a stirring speed of 300 r/min at 25 °C for 1 h, or stated otherwise. After filtration, the leach residue was dried and analyzed, while the filtrate was treated for the determination of ionic concentrations.

Table 3 Composition of $CaMoO_4$ calcine from roasting molybdenite with lime (wt.%)

MoO_3	CaO	SO_2	SiO_2	Al_2O_3	Fe_2O_3
26.4	35.8	25.4	6.17	4.27	3.26

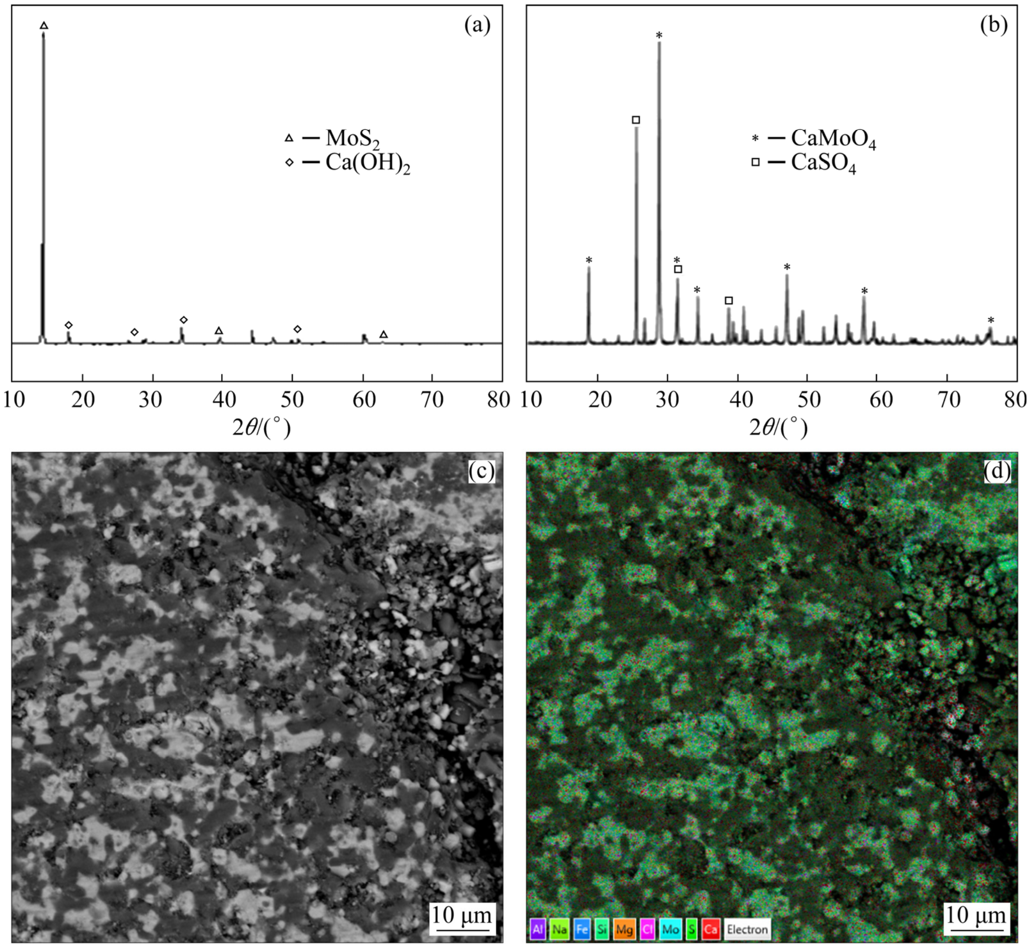

Fig. 4 XRD patterns of molybdenite before (a) and after (b) roasting, and SEM image (c) and EDS elemental map (d) of $CaMoO_4$ calcine

3.3 Sample characterization

The determination of metal concentrations in calcine and residue was conducted by ICP-OES (Inductively Coupled Plasma Optical Emission Spectrometer, Agilent 5100, USA) via acid dissolution. The distribution of elements in micro area of calcine and residue was mapped by means of SEM−EDS with polished sample solidified in epoxy resin.

3.4 Data processing

For the leaching of $CaMoO_4$, Mo^{4+} is insoluble but Mo^{6+} is soluble in acidic solutions. Therefore, the oxidation ratio of Mo can be determined by leaching the calcined $CaMoO_4$ with much excessive HCl (L/S>10:1) for more than 2 h at ~50 °C, then the Mo in leach solution and residue (dissolving 0.2 g of the residue sample by 5 mL aqua regia and 5 mL perchloric acid at a boiling temperature) can be determined by ICP-OES. The retention ratio of Mo is the ratio of Mo content in the calcined $CaMoO_4$ to the Mo content in raw molybdenite. And E is defined as the leaching efficiency of Mo and the calculation equation is shown as follows:

$$E=\frac{C_{\mathrm{Mo}}\times V}{w_0\times m_0}\times 100\% \qquad (33)$$

where C_{Mo} represents the Mo concentration in leach solution (g/L), V is volume of leach solution (L), w_0 is the Mo content in the calcined $CaMoO_4$ (%), and m_0 is the mass of the calcined $CaMoO_4$ (g).

4 Results and discussion

4.1 Effect of H^+ concentration

As shown in Fig. 5, the leaching efficiency of Mo increased with increasing concentration of H^+ for both acids. But the leaching efficiency of Mo with HCl reached up to 99% while that with H_2SO_4 only 78% under the same H^+ concentration of 2.4 mol/L. This can be attributed to the low dissolution ratio of $CaMoO_4$ embedded in $CaSO_4$ matrix and the surface coating caused by the generated $CaSO_4$ in the case of H_2SO_4 leaching, which has also been proved by the low Ca^{2+} concentration in H_2SO_4 leach solution, 2 g/L, regardless the H^+ concentration. In accord with the thermodynamic calculation results (Figs. 1(a) and (b)), the concentration of Ca^{2+} in HCl leach solution (8.5−11.9 g/L) was much higher than that in H_2SO_4 leach solution (~2 g/L) due to the low solubility of $CaSO_4$ in H_2SO_4 and the common ion effect caused by SO_4^{2-}. On the other hand, the residue ratio with HCl leaching was only 37%−55% but ~92% in the case of H_2SO_4 leaching, saving large amount of washing water and residue treatment cost. Therefore, HCl is considered as a better leachant for Mo leaching from $CaMoO_4$ calcine. And the optimal H^+ concentration was 2.4 mol/L.

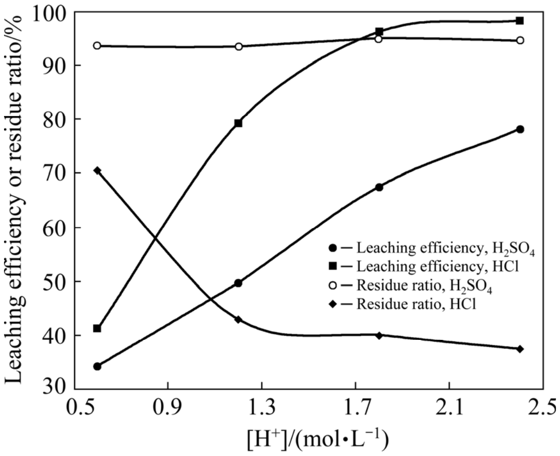

Fig. 5 Effect of H^+ concentration on dissolution of $CaMoO_4$ with sulfuric and hydrochloric acids (L/S=10:1, 25 °C, 1 h, 300 r/min)

To investigate the Mo leaching mechanism with HCl and H_2SO_4, the raw $CaMoO_4$ and leach residue particles were inserted into the polyacrylamide organic resin and polished for SEM−EDS test. As shown in Figs. 6(a) and (b), $CaMoO_4$ and $CaSO_4$ in the raw material particles are deeply embedded each other, for which the leaching of Mo requires a pre-decomposition of the $CaSO_4$ matrix. In the case of H_2SO_4 leaching, considerable amount of undissolved Mo that closely disseminated with Ca and S was found, furthermore, Ca^{2+} concentration in leach solution (~2 g/L) was low but the residue ratio was high (~92%), indicating that the undissolved $CaSO_4$ matrix hindered the release of Mo from $CaMoO_4$ calcine. In the case of HCl leaching, the Mo and S were rarely found in residue, moreover, a high Ca^{2+} in leach solution (>8.5 g/L) and a low residue ratio (<50%) were achieved at the same time. In addition, the particle size of residue with HCl leaching was smaller than that with H_2SO_4 leaching (Fig. 6(c)), and the residue ratio with HCl leaching was only half of that with H_2SO_4 leaching (Fig. 5).

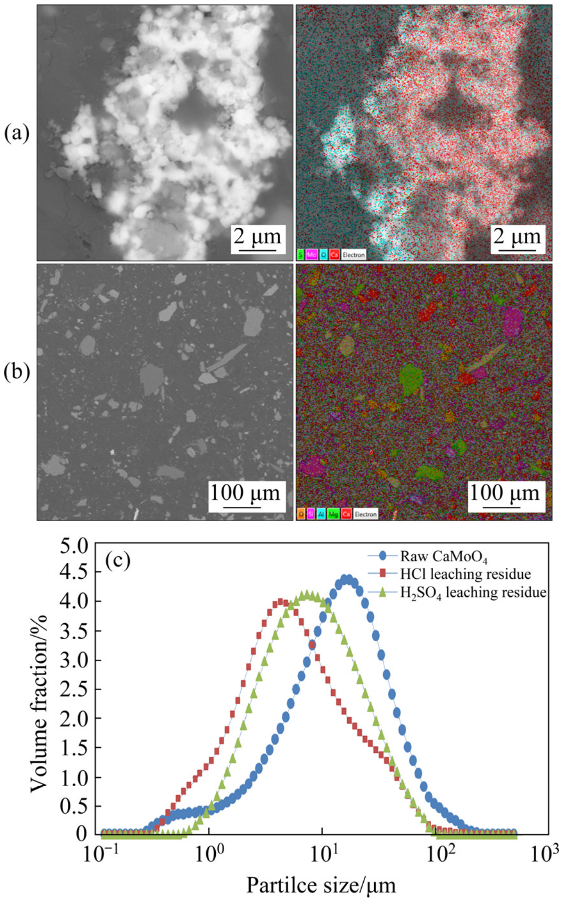

Fig. 6 SEM images and elemental maps of leaching residue from $CaMoO_4$ by H_2SO_4 (a) and HCl (b) solutions, and particle size distribution of raw $CaMoO_4$, HCl and H_2SO_4 leaching residues (c) ($[H^+]$=1.5 mol/L, L/S=10:1, 1 h, 300 r/min, 25 °C)

4.2 Effect of leaching time

The effect of leaching time on the decomposition of $CaMoO_4$ with HCl and H_2SO_4 is shown in Fig. 7(a). The leaching efficiency of Mo with HCl reached 98.6% in 45 min, indicating a fast leaching kinetics. However, in the case of H_2SO_4 leaching, only 85% of Mo leaching efficiency was obtained in 120 min. Figure 7(b) demonstrated that the concentration of Ca^{2+} in the leach solution with H_2SO_4 leaching slightly decreased with the increase of time and maintained stable around 2 g/L, while that with HCl leaching reached 12 g/L after 30 min, indicating that HCl significantly alleviated the surface wrapping of $CaMoO_4$ particles.

In conclusion, the leaching of $CaMoO_4$ with HCl exhibited a much better recovery of Mo and faster leaching kinetics than that with H_2SO_4. Therefore, the leaching system with HCl was selected for subsequent experiment.

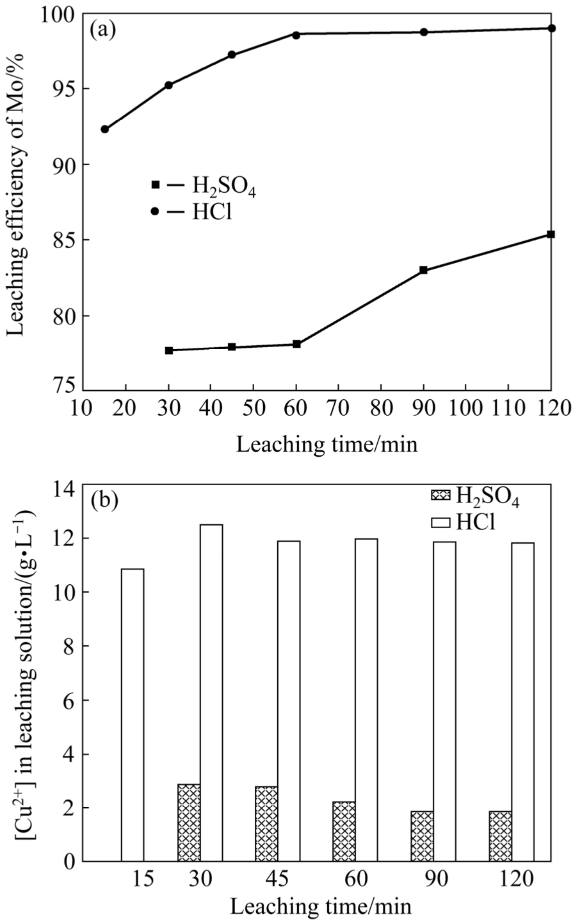

Fig. 7 Effect of leaching time on Mo leaching efficiency with H_2SO_4 and HCl (a), and $[Ca^{2+}]$ in leaching solution versus leaching time (b) ($[H^+]$=2.4 mol/L, L/S=10:1, 25 °C, 300 r/min)

4.3 Effect of temperature, L/S ratio, stirring speed and particle size

Some other conditional experiment results are plotted in Fig. 8. It was found that the leaching efficiency of Mo was all above 98% in the whole tested temperature range and reached the maximum value of 99.7% at 50 °C (Fig. 8(a)). For industrial operation, the highest leaching efficiency of Mo can be reached by self-heating of calcine in a sealed reactor without energy applying (at 50 °C). From the perspective of energy saving, room temperature was considered as the optimal initial leaching temperature.

Figure 8(b) demonstrated that the leaching efficiency of Mo increased from 83% to 97.5% with the increase in L/S ratio from 3:1 to 5:1, which can be attributed to the enhancement of both H_2MoO_4 and $CaSO_4$ dissolution. In fact, it is better to maintain HCl concentration at a relatively low level

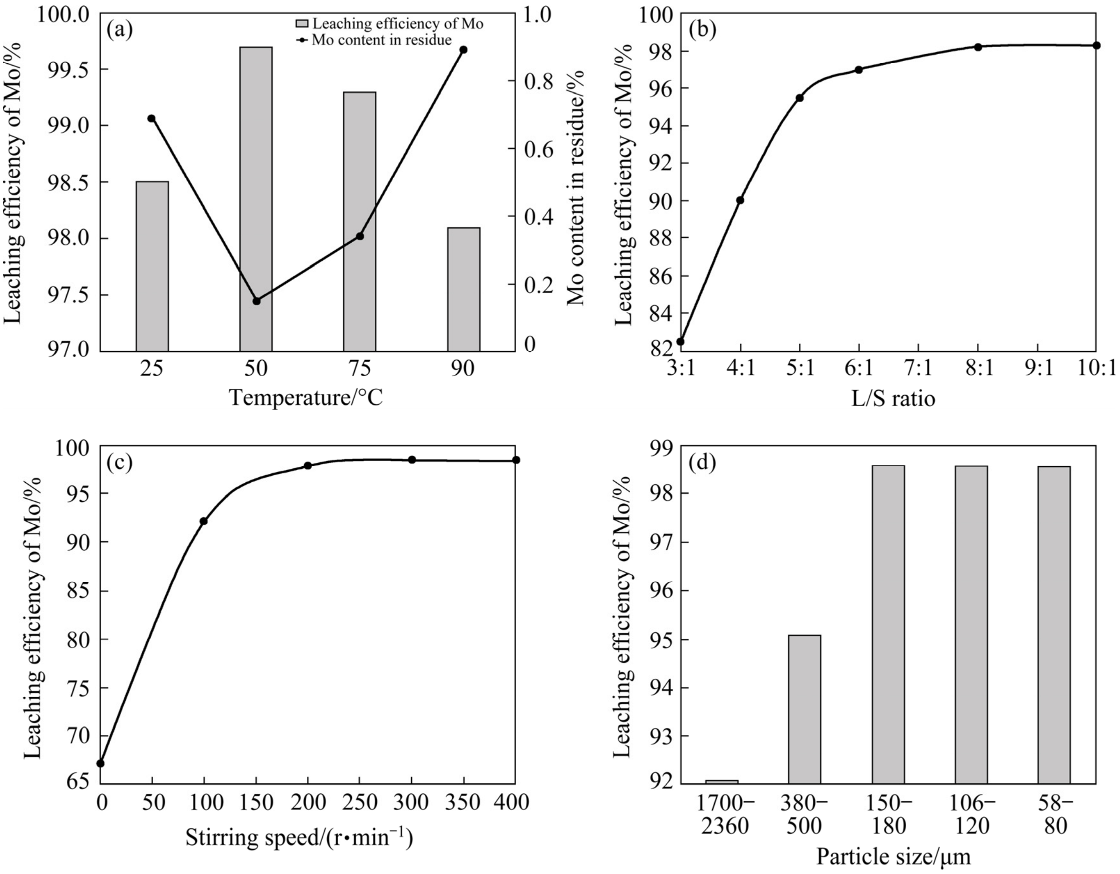

Fig. 8 Effect of temperature (L/S=5:1, 300 r/min, 74 μm) (a), L/S ratio (50 °C, 300 r/min, 74 μm) (b), stirring speed (L/S=5:1, 50 °C, 74 μm) (c), and particle size (L/S=5:1, 300 r/min, 50 °C) (d) on leaching efficiency of Mo from $CaMoO_4$ with 2.4 mol/L HCl for 1 h

(<3 mol/L) to reduce the volatilization of HCl and to regenerate HCl. Then, L/S ratio of 10:1 was adopted.

As shown in Fig. 8(c), the leaching efficiency of Mo increased obviously when the stirring speed was less than 100 r/min, indicating a diffusion controlled process. Further increase in stirring speed to 300 r/min increased the leaching efficiency of Mo to 98.5% and 300 r/min was then selected as optimum stirring speed. Known from (Fig. 8(d)), 150−180 μm (80−100 mesh) particle size was considered as the optimum values. Then, an excellent leaching efficiency of Mo, up to 99.7%, was achieved under the optimal conditions of leaching $CaMoO_4$ calcine with an L/S ratio of 10:1 by 2.4 mol/L HCl at a stirring speed of 300 r/min and 50 °C for 1 h, while the residue ratio was only 45%.

4.4 Effect of Ca^{2+} concentration

As shown in Fig. 3, an increasing concentration of Ca^{2+} in $CaCl_2$ solution significantly decreased the solubility of $CaSO_4$. To investigate the effect of Ca^{2+} concentration on the leaching efficiency of Mo, $CaCl_2$ was added into the leachant. The experimental results (Table 4) demonstrated that the increase of Ca^{2+} concentration decreased the leaching efficiency of Mo in a small quantity. According to the thermodynamic analysis of $CaSO_4$−$CaCl_2$−HCl−H_2O system, the increase of Ca^{2+} concentration reduced the solubility of $CaSO_4$, leading to an increase of undissolved $CaMoO_4$ covered by $CaSO_4$. But under other proper leaching conditions, most of the uncovered $CaMoO_4$ was dissolved, leaving a small amount of the inclusive $CaMoO_4$ in $CaSO_4$ particle bodies. Then, an increase concentration resulted in a decrease dissolution of $CaSO_4$ and retarded the leaching of the $CaMoO_4$ entrained in the $CaSO_4$ particles.

4.5 Cycle leaching of Mo from molybdenite with HCl

Based on investigations above, combined with our previous studies on the direct solvent extraction

Table 4 Effect of Ca^{2+} concentration on Mo leaching with HCl (2.4 mol/L HCl, L/S=10:1, 25 °C, 1 h, 300 r/min)

Ca^{2+} addition/ $(g\cdot L^{-1})$	Residue mass/g	Mo content in residue/wt.%	Leaching efficiency of Mo/%	Ca^{2+} concentration in leachate/$(g\cdot L^{-1})$	SO_4^{2-} concentration in leachate/$(g\cdot L^{-1})$
0	7.5	0.79	98.3	12.3	13.6
5.41	9.2	0.75	98	14.9	8.44
9.01	10.8	0.65	98	15.9	2.37
18.02	10.9	0.71	97.8	24.8	2.16

of Mo from HCl leach solutions [17], a cycle leaching process of Mo from $CaMoO_4$ with HCl was proposed (Fig. 9). The whole process includes initial leaching, solvent extraction, HCl regeneration from raffinate and the cycle leaching of Mo from molybdenite by the regenerated HCl solution.

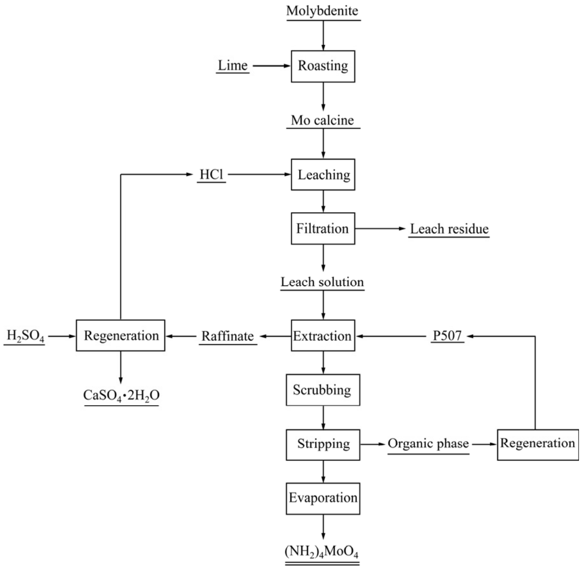

Fig. 9 Proposed flowsheet of recovering Mo from $CaMoO_4$

In this process, molybdenite is firstly roasted with lime following by HCl leaching. Then, Mo in leach solution is directly extracted by 2-ethylhexyl phosphonic acid mono-2-ethylhexyl ester (P507 or HEHEHP) via 4-stage counter current extraction and stripped by ammonia. The obtained $(NH_4)_2MoO_4$ solution is evaporated and crystallized to produce pure ammonium molybdate. The raffinate, $CaCl_2$ solution, is regenerated by H_2SO_4 to recycle the leaching agent (HCl) and to generate a by-product of pure calcium sulphate dihydrate.

To examine the recovery of Mo in each operation in the cycle leaching process, seven cycles were conducted and the obtained data are shown in Fig. 10 and Table 5. It was found that excellent leaching efficiency of Mo about 99%, high extraction efficiency of Mo above 95% and good regeneration efficiency of HCl ranging in 95%−98% (except the initial one) were achieved.

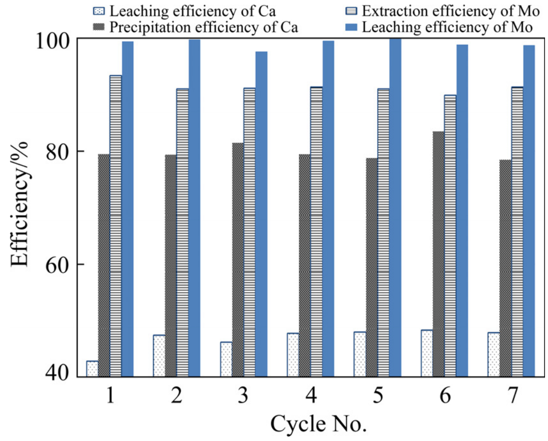

Fig. 10 Cycle leaching of Mo from $CaMoO_4$ with HCl (Leaching: 2.4 mol/L HCl, L/S=10:1, 50 °C, 1 h, 300 r/min; Solvent extraction: 30% P507, A/O=2.86:1, 25 °C, 7 min, 250 r/min; HCl regeneration: 12 mol/L H_2SO_4, $n(H_2SO_4)/n(Ca)$=0.80:1, 25 °C, 2 h, 180 r/min)

Furthermore, in the cycle leaching process, the separation coefficient of Mo to impurities ranged from $10^{3.90}$ to $10^{5.92}$, producing a high pure ammonium molybdate product which meets the Chinese National Standard of the second-grade MSA [29]. The obtained by-product, $CaSO_4\cdot 2H_2O$ (XRD pattern shown in Fig. 11), with a purity ranging from 99.0% to 99.3% and whiteness more than 91° can be directly used as the raw material for building materials [30].

Compared with the traditional H_2SO_4 leaching process of $CaMoO_4$ calcine, the passivation of undissolved $CaMoO_4$ calcine particles is eliminated and then the Mo recovery is significantly increased, the mass of waste leach residue is significantly reduced and the sulphur is converted as the by-product of pure $CaSO_4\cdot 2H_2O$ (gypsum). The proposed process is considered as a green and high efficient process.

Table 5 Co-extraction efficiency of Ca and loss of Mo in $CaSO_4 \cdot 2H_2O$ by-product

Cycle No.	Co-extraction efficiency of Ca/%	Loss of Mo/%
1	0.73	0.001
2	0.61	0.002
3	0.63	0.001
4	0.43	0.003
5	0.1	0.002
6	0.63	0.002
7	0.33	0.002

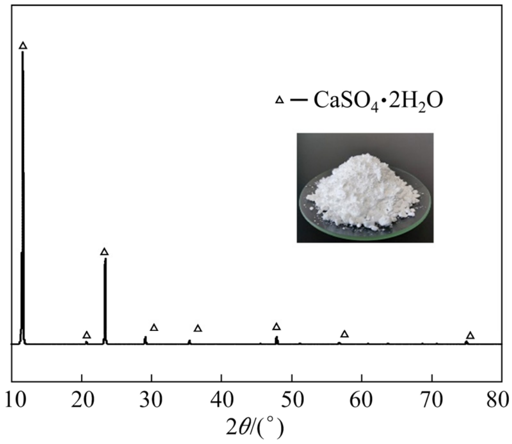

Fig. 11 XRD pattern of by-product of calcium sulphate dehydrate

5 Conclusions

(1) The thermodynamic equilibrium diagrams of $CaMoO_4-CaSO_4-H_2SO_4-H_2O$, $CaMoO_4-HCl-H_2O$ and $CaSO_4-CaCl_2-HCl-H_2O$ solution systems at 298 K were established for the direction of the development of Mo leaching process from $CaMoO_4$ calcine.

(2) HCl showed a superior leaching performance than H_2SO_4 on the decomposition of $CaMoO_4$ due to the elimination of the passivation caused by $CaSO_4$ and H_2MoO_4. High Mo leaching efficiency of 99.7% was achieved by decomposing $CaMoO_4$ calcine with 2.4 mol/L HCl at L/S ratio of 10:1 and 50 °C for 60 min.

(3) HCl cycle leaching process simultaneously recovering both Mo and Ca from the $CaMoO_4$ calcine was developed, and the 7 cycles leaching results showed an excellent overall recovery of Mo. The proposed process possessed a good industrial application prospect due to its excellent performance, water recycling and residue reduction.

Acknowledgments

This work was financially supported by the Joint Fund for Nuclear Technology Innovation Sponsored by the National Natural Science Foundation of China and the China National Nuclear Corporation (No. U2067201).

References

[1] ALEKSANDROV P V, MEDVEDEV A S, MILOVANOV M F, IMIDEEV V A, KOTOVA S A, MOSKOVSKIKH D O. Molybdenum recovery from molybdenite concentrates by low-temperature roasting with sodium chloride [J]. International Journal of Mineral Processing, 2017, 161: 13−20.

[2] MAHANDRA H, SINGH R, GUPTA B. Development of a hydrometallurgical route for the recovery of molybdenum from spent hydrodesulphurization catalyst using Cyphos IL 104 [J]. Journal of Industrial and Engineering Chemistry, 2018, 65: 213−223.

[3] WANG Lu, ZHANG Gou-hua, DANG Jie, CHOU K C. Oxidation roasting of molybdenite concentrate [J]. Transactions of Nonferrous Metals Society of China, 2015, 25: 4167−4174.

[4] PINTO I S S, SOARES H M V M. Recovery of molybdates from an alkaline leachate of spent hydrodesulphurisation catalyst-proposal of a nearly-closed process [J]. Journal of Cleaner Production, 2013, 52: 481−487.

[5] ZENG Li, CHENG Chu-yong. A literature review of the recovery of molybdenum and vanadium from spent hydrodesulphurisation catalysts. Part I: Metallurgical processes [J]. Hydrometallurgy Amsterdam, 2009, 98: 1−9.

[6] JUNEJA J M, SINGH S, BOSE D K. Investigations on the extraction of molybdenum and rhenium values from low grade molybdenite concentrate [J]. Hydrometallurgy, 1996, 41: 201−209.

[7] SWINKELS P L J, WEIJDEN R D, AJAH A N, ARIFIN Y, LOE H L, MANIK M H, SIRISKI I, REUTER M A. Conceptual process design as a prerequisite for solving environmental problems: A case study of molybdenum removal and recovery from wastewater [J]. Minerals Engineering, 2004, 17: 205−215.

[8] ZHANG Di, LIU Yun-qing, HU Qi-zhao, KE Xin-quan, YUAN Sheng-hua, LIU Shi-jun, JI Xiao-bo, HU Jiu-gang. Sustainable recovery of nickel, molybdenum, and vanadium from spent hydroprocessing catalysts by an integrated selective route [J]. Journal of Cleaner Production, 2020, 252: 119763.

[9] JIANG Kai-xi, WANG Yu-fang, ZOU Xiao-ping, ZHANG Lei, LIU San-ping. Extraction of molybdenum from molybdenite concentrates with hydrometallurgical processing [J]. JOM, 2012, 64: 1285−1289.

[10] LASHEEN T A, EL-AHMADY M E, HASSIB H B, HELAL A S. Molybdenum metallurgy review: Hydrometallurgical routes to recovery of molybdenum from ores and mineral raw materials [J]. Mineral Processing and Extractive Metallurgy Review, 2015, 36: 145−173.

[11] SONG Jian-zheng, ZHANG Yong-qiang. Experimental study on leaching calcium molybdate with sodium carbonate solution [J]. Hebei Chemical Engineering and Industry, 2008, 31: 14−16. (in Chinese)

[12] XIA Wen-tang, ZHAO Zhong-wei, LI Hong-gui. Thermodynamic analysis on sodium carbonate decomposition of calcium molybdenum [J]. Transactions of Nonferrous Metals Society of China, 2007, 17: 145−173.

[13] PAN Mao-sen, ZHU Yun. Experimental study on leaching molybdenum at high pressure from calcium molybdate [J]. China Molybdenum Industry, 2005, 20: 23−25 (in Chinese)

[14] ZHANG Gang, ZHAO Zhong-wei, CAO Cai-fang, HUANG Shao-bo. Thermodynamic analysis on phosphate decomposition of calcium molybdate [J]. Journal of University of Science and Technology Beijing, 2009, 31: 1394−1399.

[15] SHALCHIAN H, FERELLA F, BIRLOAGA I, MICHELIS I D, VEGLIÒ F. Recovery of molybdenum from leach solution using polyelectrolyte extraction [J]. Hydrometallurgy, 2019, 190: 105167.

[16] LASHEEN T A, IBRAHIM M E, HASSIB H B, HELAL A S. Recovery of molybdenum from uranium bearing solution by solvent extraction with 5-Nonylsalicylaldoxime [J]. Hydrometallurgy, 2014, 146: 175−182.

[17] XIAO Chao, ZENG Li, XIAO Lian-sheng, ZHANG Gui-qing. Solvent extraction of molybdenum (VI) from hydrochloric acid leach solutions using P507. Part I: extraction and mechanism [J]. Solvent Extraction and Ion Exchange, 2017, 35: 130−144.

[18] XIAO Chao, ZENG Li, XIAO Lian-sheng, ZHANG Gui-qing. Solvent extraction of molybdenum (VI) from hydrochloric acid leach solutions using P507. Part II: stripping and mechanism [J]. Solvent Extraction and Ion Exchange, 2017, 35: 549−562.

[19] XIA Yun, XIAO Lian-sheng, XIAO Chao, ZENG Li. Direct solvent extraction of molybdenum (VI) from sulfuric acid leach solutions using PC-88A [J]. Hydrometallurgy, 2015, 158:114−118.

[20] ILHAN S, KALPAKLI A O, KAHRUMAN C, YUSUFOGLU I. The use of Langmuir–Hinshelwood mechanism to explain the kinetics of calcium molybdate leaching in oxalic acid solution [J]. Hydrometallurgy, 2012, 127−128: 91−98.

[21] ILHAN S, KALPAKLI A O, KAHRUMAN C, YUSUFOGLU I. The use of oxalic acid as a chelating agent in the dissolution reaction of calcium molybdate [J]. Metallurgical and Materials Transactions: Part B, 2013, 44: 495−505.

[22] SINGH S, CHETTY M K, JUNEJA J M, SEHRA J C, GUPTA C K. Studies on the processing of a low grade molybdenite concentrate by lime roasting [J]. Minerals Engineering, 1988, 1: 337−342.

[23] ZOU Zhen-qiu, ZHOU Qin-jian. Recovery of molybdenum and rhenium from molybdenite concentrate in Dexing Copper Ore by lime roasting-N235 extraction method [J]. Mining and Metallurgical Engineering, 2002, 22: 79−81. (in Chinese)

[24] CHEN Xu-ling, WANG Hai-bo, GAN Min, FAN Xiao-hui, ZHANG Lin, DENG Qiong, WANG Yong, ZENG Jin-lin. Extraction of molybdenum from low grade molybdenum concentrates by calcium-based roasting and acid leaching process [J]. The Chinese Journal of Nonferrous Metals, 2015, 25: 2913−2920. (in Chinese)

[25] BURNS D T. Handbook of chemical equilibria in analytical chemistry (Volume 9) [M]. Horwood: Wiley, 1985: 151.

[26] DEAN J A. Lange's handbook of chemistry [M]. 15th ed. New York: McGraw Hill, 1999.

[27] MARINA L S, LI X H, DAVID H, HILLA S, RAPHAEL S. Solubility limits of $CaSO_4$ polymorphs in seawater solutions [J]. Desalination, 2020, 475: 114200.

[28] LI Z B, DEMOPOULOS G P. Effect of NaCl, $MgCl_2$, $FeCl_2$, $FeCl_3$, and $AlCl_3$ on solubility of $CaSO_4$ phases in aqueous HCl or HCl+$CaCl_2$ solutions at 298 to 353 K [J]. Journal of Chemical & Engineering Data, 2006, 51(2): 569−576.

[29] The China National Standardization Management Committee. Ammonium molybdate, GB/T 3460—2017 [S]. (in Chinese)

[30] XUE Wang, WEN Ni, LI Jia-jie, ZHANG Si-qi, MICHEAL H, RODRIGO P. Carbonation of steel slag and gypsum for building materials and associated reaction mechanisms [J]. Cement and Concrete Research, 2019, 125: 105893.

盐酸循环浸出强化钼酸钙焙砂分解及资源化回收钙

曾理[1,2,3]，王曼[1,2,3]，肖超[1,2,3]，巫圣喜[1,2,3]，张贵清[1,2,3]，关文娟[1,2,3]，李青刚[1,2,3]，曹佐英[1,2,3]

1. 中南大学 冶金与环境学院，长沙 410083；2. 中南大学 冶金分离科学与工程重点实验室，长沙 410083；
3. 中南大学 难选有色金属资源高效利用国家工程实验室，长沙 410083

摘　要：建立 298 K 下 $CaMoO_4-CaSO_4-H_2SO_4-H_2O$，$CaMoO_4-HCl-H_2O$ 和 $CaSO_4-CaCl_2-HCl-H_2O$ 体系的热力学平衡图。计算结果表明，硫酸钙在盐酸中的溶解度远大于在硫酸中的溶解度。从微观颗粒性质变化的角度探讨钼酸钙焙砂中钼的浸出机理。研究发现，盐酸对钼酸钙焙砂中的钼具有良好的浸出效果，这是因为盐酸能消除钼的表面包覆，并溶解嵌入硫酸钙基体中的钼。条件优化结果显示，采用 2.4 mol/L 盐酸，在液固比为 10:1 及 50 ℃条件下浸出 60 min，钼的浸出率达到 99.7%。基于此，提出一种从辉钼矿中高效绿色循环浸出钼的新工艺，消除钼的表面包覆和物理夹带，并将钼酸钙焙砂中大部分钙转化为高纯石膏副产品。

关键词：钼酸钙；钼；硫酸浸出；盐酸浸出；热力学

(Edited by Wei-ping CHEN)